

## Water Soluble Trianiline Containing Polyurethane (TAPU) as an Efficient Corrosion Inhibitor for Mild Steel

Feng Yang<sup>1</sup>, Xiangyu Li<sup>1,2</sup>, Shihui Qiu<sup>2</sup>, Wenru Zheng<sup>2</sup>, Haichao Zhao<sup>2,\*</sup>, Liping Wang<sup>2,\*</sup>

<sup>1</sup> School of Materials Science and Engineering, Shenyang University of Chemical Technology, Shen Yang, 110142, China

<sup>2</sup> Key Laboratory of Marine Materials and Related Technologies, Zhejiang Key Laboratory of Marine Materials and Protective Technologies, Ningbo Institute of Materials Technology and Engineering, Chinese Academy of Sciences, Ningbo 315201, P. R. China.

\*E-mail: [zhaohaichao@nimte.ac.cn](mailto:zhaohaichao@nimte.ac.cn), [wangliping@nimte.ac.cn](mailto:wangliping@nimte.ac.cn)

Received: 2 March 2017 / Accepted: 23 April 2017 / Published: 12 May 2017

---

Novel trianiline containing water soluble polyurethane (TAPU) was synthesized by polymerization of polyethylene glycol, toluene diisocyanate and amine-capped aniline trimer. The influence of TAPU on the corrosion inhibition of mild steel in 1 M HCl was investigated using weight loss measurements, potentiodynamic polarization, electrochemical impedance spectroscopy (EIS). The performance of TAPU on the corrosion inhibition of mild steel was also evidenced by scanning electron microscopy (SEM), energy dispersive spectroscopy (EDS) and atomic force microscope (AFM). Results confirmed that the adsorption of TAPU on the mild steel surface and consequent inhibition of the corrosion process. The inhibition efficiency (IE%) increased with a rise in TAPU concentration, reaching a value up to 97% at a concentration of 200 mg/l. Potentiodynamic polarization curves showed that the TAPU affected both cathodic and anodic protection and was a mixed type inhibitor in HCl corrosive medium. Adsorption isotherm studies confirmed that the adsorption of TAPU on the mild steel surface in 1 M HCl solution obeyed Langmuir adsorption isotherm. EDS analysis determined the adsorption of TAPU molecules on the steel surface, and the absorbed TAPU provided an effective corrosion inhibition in 1 M HCl solution from observation of surface morphology by SEM and AFM.

---

**Keywords:** polyurethane; trianiline; acidic aqueous solution; corrosive inhibitor; mild steel

### 1. INTRODUCTION

The protection of metal against corrosion in acidic solution is of great importance in several acid-based industrial processes such as acid assisted pickling, cleaning, descaling and oil well acidizing[1, 2]. One of the most practical methods to reduce the corrosion of metal in acidic media is the use of organic inhibitors dissolved in the corrosive solution[3, 4]. Such organic inhibitors usually

contain unsaturated bonds[5], conjugated aromatic rings[6], or heteroatoms such as N, P, O, and S[7, 8], which are capable of forming barrier films on the metal surface[9-11], neutralizing hydrogen ions in the medium, or scavenging dissolved oxygen[12], etc.

As compared to small molecule corrosion inhibitors, polymers bearing heteroatoms have the advantages of better film forming capabilities, flexible viscosity and functionality, which might provide better protection of steel against corrosive media[13]. Polyaniline (PANI), a conducting polymer bearing  $\pi$ -electrons in the benzene ring and abundance of nitrogen atom in the backbone, is considered as one of most promising candidates for corrosion inhibitors[14, 15]. Polyaniline chains can interact metal to form a protective film through electrostatic adsorption, chemisorption and  $\pi$ -orbital adsorption, hence hindering the penetration of corrosive substances. True indeed, it has been demonstrated that polyaniline showed much better corrosion protection than its monomeric counterpart as determined by polarization curves. However, one obstacle to application of polyaniline as corrosion inhibitors is its extremely poor solubility of polyaniline in aqueous medium[16]. To address this issue, several acids such as dodecyl benzene sulfonic acid, polyacrylic acid, sulfonated chitosan and poly(styrene sulfonic acid) doped polyanilines have been developed as an inhibitors in acidic and saline water media[17, 18]. Other methods include incorporation of alkyl substituents, sulfonic acid in the polyaniline side chains[18, 19], or by copolymerization with a soluble monomer such as 4-amino-3-hydroxy naphthalene-1-sulfonic acid to achieve the processable PANi.

Quite different from PANi, oligoanilines possess similar electroactivity to that of PANi, while exhibiting excellent solubility and precise molecular structure[20]. Several types of oligoaniline-containing soluble and electroactive polymers have been developed such as electroactive polyurethane[21], polyimide[22], poly(lactic acid)[23], etc. In this work, we aim to synthesize a new water-soluble trianiline-containing polyurethane (TAPU) and investigated the corrosion inhibitive effect on mild steel in HCl medium by using weight loss experiments, open-circuit potential (OCP), potentiodynamic polarization, SEM images, EDS and AFM analysis.

## 2. EXPERIMENTAL SECTION

### 2.1. Materials

Polyethyleneglycol diol (PEG2000), stannous octoate, hexane and anhydrous tetrahydrofuran (THF) were purchased from Aladdin Industrial Corporation. Toluene diisocyanate (TDI) were purchased from Tokyo Chemical Industry. Trianiline (TA) was prepared according to the literature[24]. Acetone and HCl were purchased from Sinopharm Chemical Reagent Co. Ltd. All chemicals and solvent were used as received without further purification. Mild steel specimens with compositions C (1.39%), Mn (0.29%), Al (0.18%) were used. The mild steel plates were cut into (1 cm  $\times$  1 cm  $\times$  0.1 cm) coupons for mass loss test, polarization and electrochemical impedance test. They were polished using 180, 400, 800 and 1500-grit sand papers and degreased with acetone before being immersed in the acid solution. The acidic medium was prepared by dilution of AR grade HCl (35%, density 1.2).

## 2.2. Synthesis of trianiline-containing water soluble polyurethane (TAPU)

Scheme 1 showed the synthetic route for the preparation of trianiline containing polyurethane (TAPU), polyethylene glycol containing PU prepolymer was first prepared by dissolving polyethylene glycol diol (30 g, 15 mmol), TDI (4.8 g, 30 mmol), stannous octoate (0.1 mL) in 200 mL THF under magnetic stirring. After the mixtures were heated to 60 °C and maintained for 3 h, trianiline (5.4 g 15 mmol) was added in one-pot, and the mixtures were further reacted for another 3 h. The as-prepared product was precipitated into a large amount of hexane, filtered and dried in a vacuum to a constant weight to obtain oligoaniline-containing polyurethane (36.1 g).

## 2.3 Characterization

FTIR spectrum of the pure compound was recorded on NICOLET 6700 spectrometer. UV-vis spectrum was recorded between 300 and 800 nm using Lambda 950 spectroscope. The morphology of the uninhibited and inhibited mild steel surface was investigated using atomic force microscopy (AFM Dimension3100V). The surface morphology and energy dispersive spectroscopy (EDS) of specimens were performed on FEI Quanta FEG 250 scanning electronic microscope (SEM). For atomic force microscope (AFM) analysis, the mild steel specimens of size 1 cm × 1 cm × 0.1 cm were immersed in the test solutions in the absence and presence of inhibitors for 2 h at room temperature. Then the specimens were taken out from the solution, cleaned with distilled water, dried, and used for AFM.

## 2.4 Weight loss measurements

Steel specimens were immersed in 100 mL of 1 M HCl with and without the TAPU for 24 h at room temperature. The specimens were then rinsed with water and acetone, and dried. The cleaned specimens were weighed and the inhibitive efficiency (IE%) of the specimens with various concentrations of TAPU was obtained by:

$$IE\% = \frac{W_0 - W}{W_0} \times 100\%$$

where  $W_0$  and  $W$  are the mass values in the absence and presence of the inhibitor.

## 2.5 Electrochemical impedance spectroscopy studies

Electrochemical impedance tests were performed in a conventional three-electrode cell assembled with mild steel working electrode with 2.5 cm<sup>2</sup> platinum foil as counter electrode, and saturated calomel electrode (SCE) as the reference electrode. The measurements were performed with CHI-660E, Chenhua, Shanghai. The EIS measurements were performed at steady open circuit potential over a frequency range of 100 kHz to 10 mHz with amplitude of 10 mV. The double layer capacitance ( $C_{dl}$ ) and the charge transfer resistance ( $R_{ct}$ ) were calculated from Nyquist plots by means of ZsimpWin software fitting. As  $R_{ct}$  was inversely proportioned to the corrosion current density, it was used to determine the inhibitor efficiency IE% and surface coverage ( $\theta$ ) from the relationship below:

$$IE\% = \frac{R_{ct} - R_{ct}^0}{R_{ct}} \times 100\%$$

$$\theta = IE\% / 100$$

$R_{ct}$  and  $R_{ct}^0$  are charge transfer resistance in the presence and absence of the inhibitors.

Polarization curves were performed with 0.2 mV/s scan rate and started from a potential of -250 mV to +250 mV vs OCP. The immersion time before measurements was 2 h. The inhibition efficiency, IE%, was calculated from the following equation:

$$IE\% = \frac{i_{corr}^0 - i_{corr}}{i_{corr}^0} \times 100\%$$

$i_{corr}^0$  and  $i_{corr}$  signify the corrosion current density in the absence and presence of inhibitors.

## 2.6 Adsorption isotherm

The adsorption of organic inhibitor could be analyzed quantitatively by the adsorption isotherms. The isothermal adsorption equation was as follows:

$$\frac{c_{inh}}{\theta} = \frac{1}{K_{ads}} + c_{inh}$$

$c_{inh}$  is the inhibitor concentration and  $K_{ads}$  is the equilibrium constant for the adsorption-desorption process.

The equilibrium constant ( $K_{ads}$ ) was related to the standard free energy of adsorption ( $\Delta G_{ads}$ ) as given below:

$$K_{ads} = \frac{1}{55.5} \exp \left( - \frac{\Delta G_{ads}}{RT} \right)$$

where R is the gas constant and T is the absolute temperature (K). The value of 55.5 is the concentration of water in solution in mol L<sup>-1</sup>.

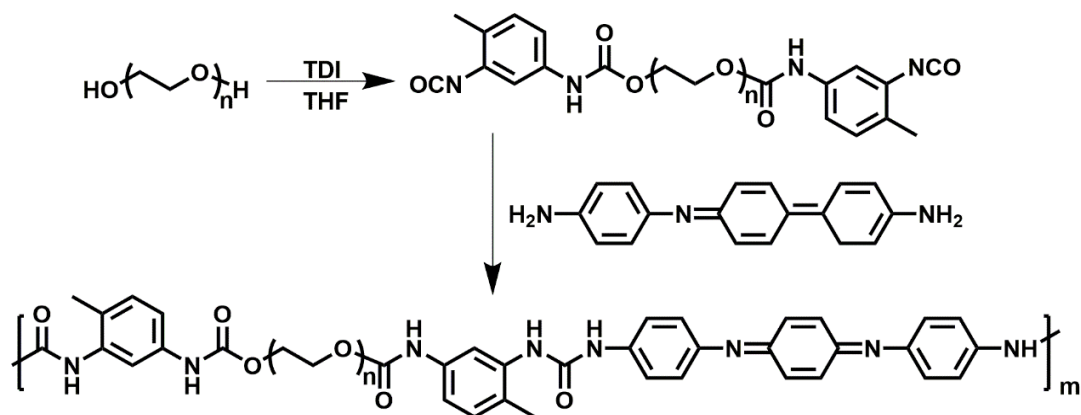
## 3. RESULTS AND DISCUSSION

### 3.1. Synthesis and characterization of water soluble trianiline containing polyurethane (TAPU)

The synthesis of trianiline containing water soluble polyurethane was shown in Scheme 1. The polymerization involved the formation of prepolymer at the initial stage by reaction between polyethylene glycol and toluene diisocyanate, followed by chained extended reaction using amine capped aniline trimer. The structure of TAPU was characterized by FTIR and UV-vis spectroscopy. In the FTIR spectrum shown in Figure 1, the characteristic peaks at 3423 cm<sup>-1</sup> and 1713 cm<sup>-1</sup> were corresponded to the stretching -C=O and N-H from urea group of TAPU[25, 26]. The peaks at 2885 cm<sup>-1</sup> and 1466 cm<sup>-1</sup> represented C-H stretching and bending vibrations[19]. Furthermore, the characteristic peaks observed at 964 cm<sup>-1</sup> and 1113 cm<sup>-1</sup> were attributed to C-O-C deformation and

stretching vibrations[27]. The peaks at  $1508\text{ cm}^{-1}$  and  $1600\text{ cm}^{-1}$  represented stretching of the quinonoid and benzenoid ring, respectively. In addition the peak at  $1340\text{ cm}^{-1}$  corresponded to C–N stretching vibration[28, 29].

Figure 2 showed the UV-vis spectrum of TAPU. It exhibited the absorption at 318 and 582 nm, which were associated with  $\pi$ - $\pi^*$  transition of benzene ring and benzenoid to quinoid transition of aniline trimer in TAPU main chain[27]. Overall, the FTIR and UV-vis studies confirmed the formation of polyurethane containing water soluble polyethylene glycol segment and electroactive oligoaniline segment.



**Scheme 1.** Synthetic route for the synthesis of water soluble trianiline-containing polyurethane.

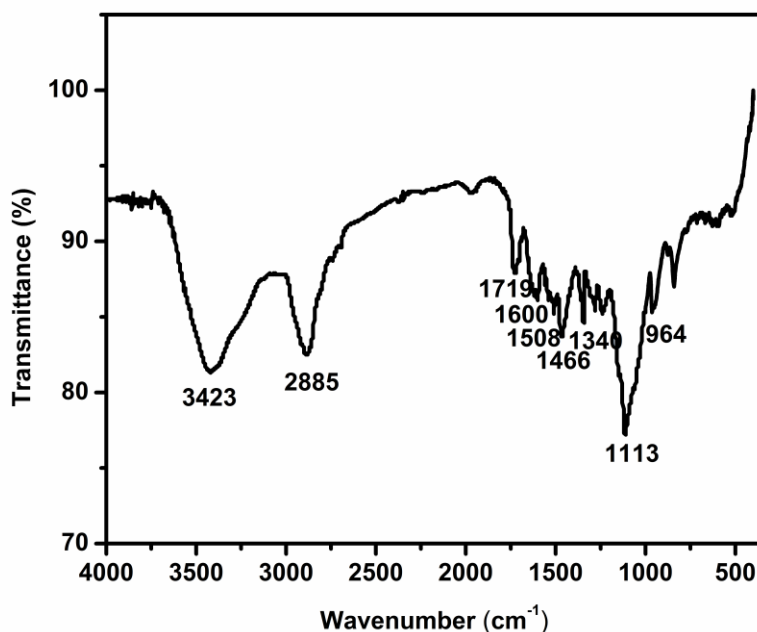


**Figure 1.** FTIR spectrum of TAPU.

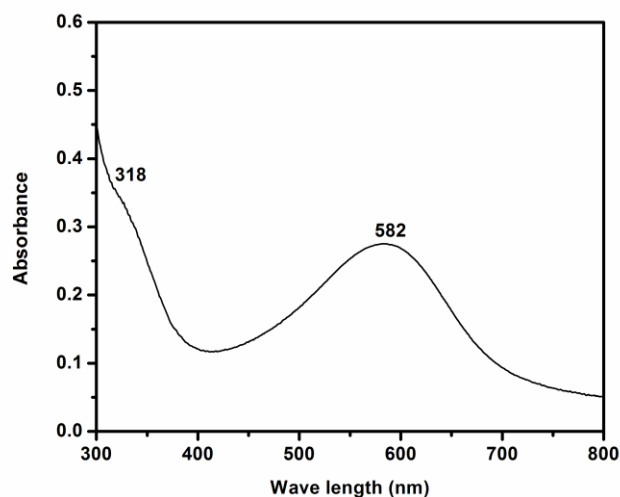


Figure 2. UV-vis spectrum of TAPU.

### 3.2 Potentiodynamic polarization

The inhibiting effects of TAPU on mild steel corrosion were investigated using mass loss and polarization curves. The potentiodynamic polarization curves obtained from mild steel in 1 M HCl as a function of TAPU concentration were shown in Figure 3. The electrochemical parameters including corrosion potential ( $E_{corr}$ ), corrosion current density ( $i_{corr}$ ), cathodic Tafel slopes ( $\beta_c$ ), anodic Tafel slopes ( $\beta_a$ ) and the inhibition efficiency (IE%) obtained from the polarization measurements were listed in Table 1.

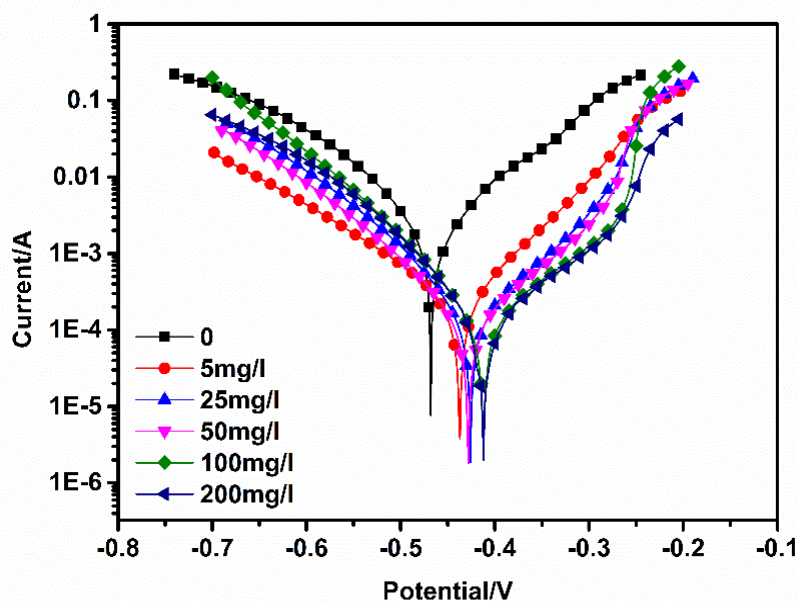


Figure 3. Polarization curves for mild steel in 1 M HCl containing different concentration of TAPU.

**Table 1.** Electrochemical parameters and inhibition efficiencies of mild steel in 1 M HCl in the absence and presence of different concentrations of TAPU at RT.

Concn. (mg/l)	$E_{corr}$ (mV)	$i_{corr}$ ( $\mu\text{A cm}^{-2}$ )	$\beta_a$ (mV dec <sup>-1</sup> )	$\beta_c$ (mV dec <sup>-1</sup> )	Inhibition efficiency (IE%)	
					Polarization	Weight loss
0	-468	2261	82.09	94.02		
5	-437	242.6	118.86	86.36	89.27	86.82
25	-426	141.5	113.43	140.34	93.74	91.80
50	-426	132.6	101.44	123.05	94.14	94.61
100	-412	78.29	281.24	124.79	96.53	96.41
200	-412	69.3	210.63	122.29	96.93	97.01

It was observed that the  $E_{corr}$  values in presence of TAPU inhibitor were slightly more positive and the deviation of  $E_{corr}$  was within 85 mV, demonstrating that the TAPU acted as a mixed type inhibitor by simple blocking the steel surface[30]. Moreover, the decrease in  $i_{corr}$  with the increase in TAPU concentration suggested that the presence of TAPU retarded the dissolution of mild steel electrodes by decelerating the evolution of the cathodic hydrogen[31]. The inhibition efficiency (IE%) obtained from the polarization and gravimetric measurements showed that the inhibition efficiencies increased with the increase in TAPU concentrations and the inhibitive efficiency reached 97% at the concentration of 200 mg/l of TAPU in 1 M HCl. In addition, the values of  $\beta_c$  and  $\beta_a$  changed with the addition of TAPU, implying that TAPU inhibited both the anodic and cathodic reactions[32].

### 3.3 Electrochemical Impedance Spectroscopy

Electrochemical impedance spectroscopy was used to investigate the corrosion and adsorption phenomena. Nyquist plots of mild steel in 1 M HCl solution in the absence and presence of various concentrations of TAPU were given in Figure 4. The Nyquist impedance plots were fitted by using a simple circuit model including solution resistance ( $R_s$ ), charge transfer resistance ( $R_{ct}$ ), and double layer capacitance ( $C_{dl}$ ), as shown in Table 2. It was observed that the diameters of the capacitive loop and  $R_{ct}$  values increased with the increase of the concentrations of TAPU, while the values of  $C_{dl}$  decreased with the increase of TAPU concentration. The increase in  $R_{ct}$  and decrease in  $C_{dl}$  values were attributed to formation of a protective layer via absorption of TAPU polymers on the metal surface, which decreased electrotransfer between metal surface and electrolyte and local dielectric constant[31, 33].

The Bode plots for mild steel immersed in 1 M HCl in the absence and various concentrations of TAPU at its open potential circuit were shown in Figure 5. It was observed that impedance values at low frequencies in the presence of TAPU were larger than that without inhibitor and the values increased with increasing in the TAPU concentrations. These results confirmed that the corrosion process was retarded and the higher protection efficiency with the higher concentrations of TAPU [34, 35].

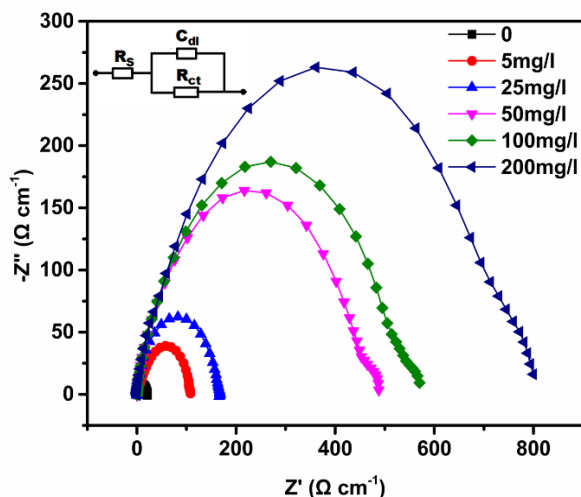


**Figure 4.** Nyquist plots for mild steel in 1 M HCl in the absence and presence of various concentrations of TAPU.

**Table 2.** Impedance data and surface coverage for mild steel in 1 M HCl in the absence and presence of various concentrations of TAPU.

Concn. (mg/l)	$R_{ct}$ ( $\Omega\text{cm}^2$ )	$C_{dl}$ ( $\mu\text{Fcm}^{-2}$ )	IE%	$\theta$
0	20.01	380.75		
5	108.87	361.23	81.62	0.82
25	159.96	78.64	87.48	0.87
50	452.51	54.43	95.58	0.95
100	520.17	54.58	96.15	0.96
200	737.42	81.58	97.28	0.97

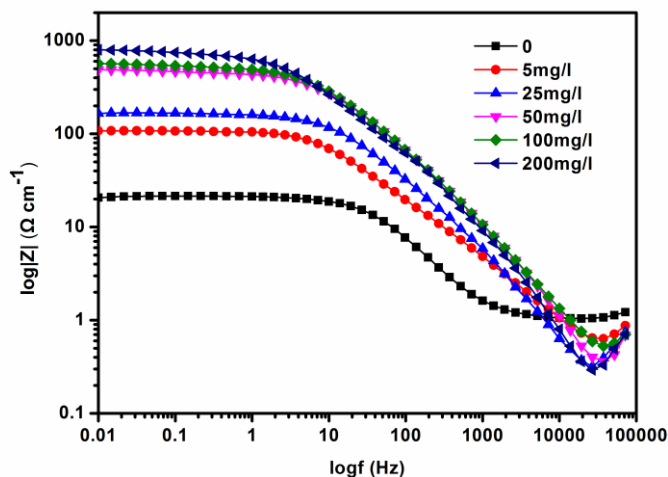


**Figure 5.** Bode plots for mild steel in the 1 M HCl solution containing different concentrations of TAPU.



### 3.4 Adsorption isotherm

Adsorption isotherm is one of the most efficient way to study quantitatively the adsorbed inhibitor layer on the metal surface[31, 36]. Figure 6 showed the inhibitor concentration ( $C_{inh}$ ) plotted against  $C_{inh}/\theta$  of the TAPU. It was found that a straight line was obtained by plotting  $C_{inh}/\theta$  vs.  $C_{inh}$ , demonstrating that the adsorption of TAPU on the mild steel surface obeyed the Langmuir adsorption isotherm[1, 31]. The standard free energy ( $\Delta G_{ads}$ ) of adsorption were calculated by equilibrium constants ( $K$ )[3]. In general,  $\Delta G_{ads}$  values up to  $-20 \text{ kJ}\cdot\text{mol}^{-1}$  are identified to physisorption and  $\Delta G_{ads}$  values are more negative than  $-40 \text{ kJ}\cdot\text{mol}^{-1}$  corresponding to chemisorptions[37]. The calculated value of  $\Delta G_{ads}$  in present work was  $-25.83 \text{ kJ}\cdot\text{mol}^{-1}$  which was between the threshold values for physical adsorption and chemical adsorption, indicating that the adsorption process of TAPU at mild steel surface were both the physical as well as chemical adsorption[34, 38].

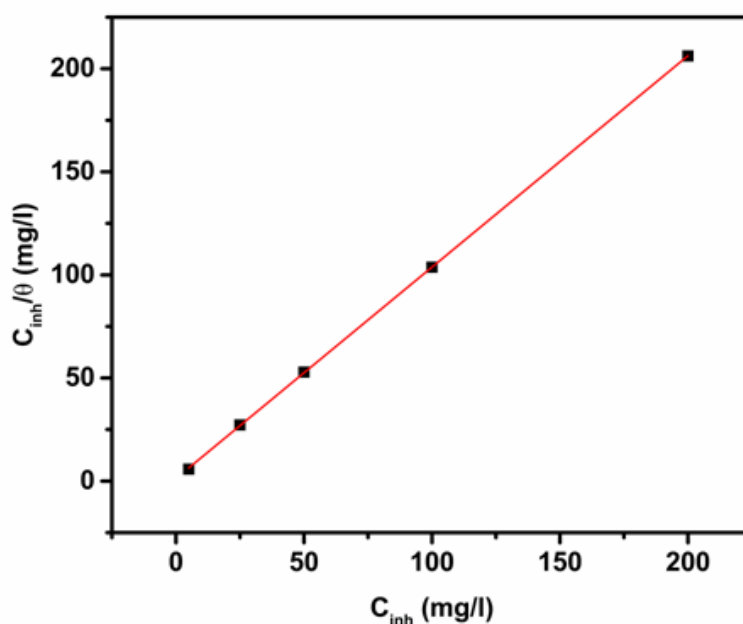


**Figure 6.** Langmuir adsorption plots for mild steel in 1 M HCl at different concentration of TAPU.

### 3.5 Surface morphology

The morphology of the mild steel specimens in the absence and presence of TAPU were investigated by SEM. As shown in Figure 7, the polished steel surface exhibited a smooth surface with some small nicks spread over, whereas the specimen showed corroded and damaged morphology with many pits and cracks due to dissolution of steel in acidic solution. Obviously, the specimens in presence of TAPU exhibited much smoother surface due to reduced corrosion rate by the surface coverage of inhibitor molecules. The absorbed TAPU on the steel surface acted as protecting film to provide corrosion protection by reducing the mass transfer of reactants between the acidic solution and steel surface[39].

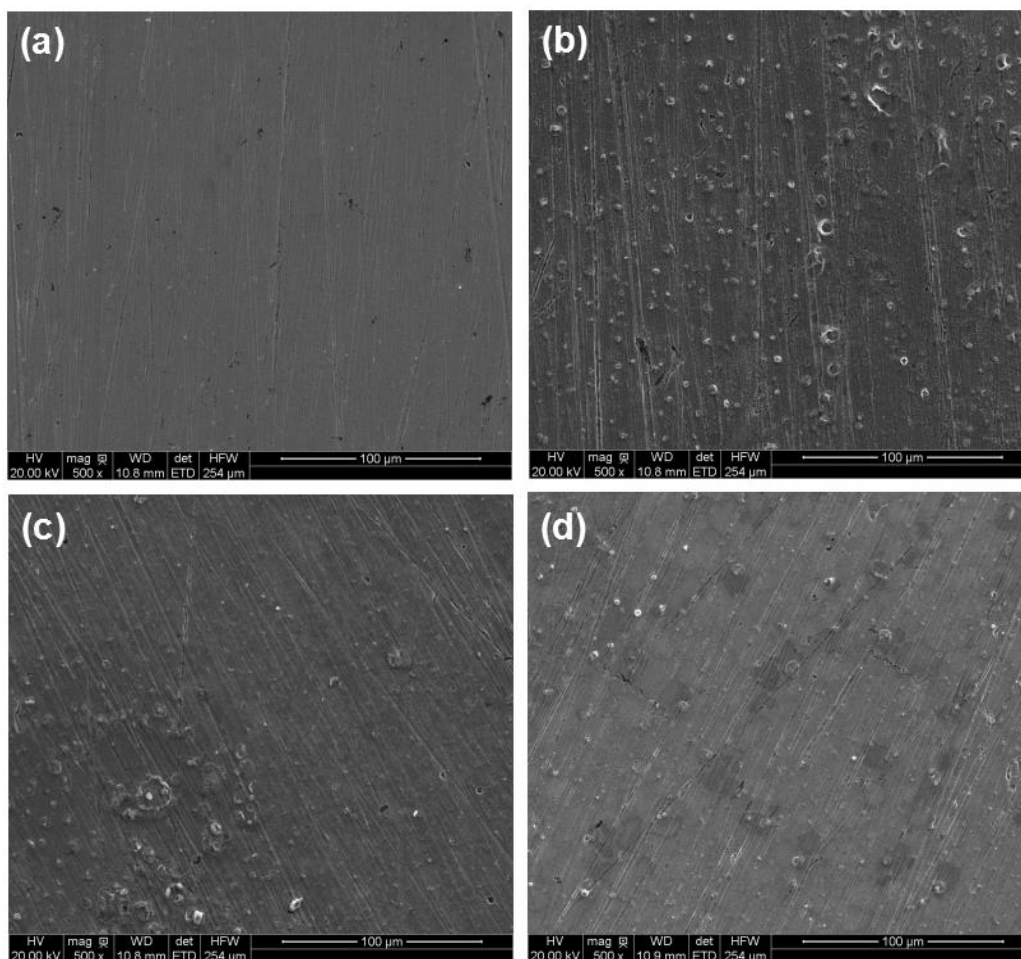


**Figure 7.** SEM micrographs on the surface of the mild steel specimens in 1 M HCl for 2 hours, (a) polished, (b) after immersion without inhibitor, (c) with 5 mg/l TAPU, (d) with 200 mg/l TAPU.

Atomic Force Microscopy was employed to further examine the influence of TAPU on the corrosion of mild steel in 1 M HCl acid solution[37]. As shown in Figure 8, it was apparent that the specimen immersed in acid solution exhibited much more rougher surfaces compared to the polished steel, as well as those immersed in the acid solution containing 5 and 200 mg/l TAPU. The average roughness ( $R_a$ ), root-mean-square roughness ( $R_q$ ) and the maximum peak-to-valley height values from the AFM image analysis were listed in Table 3. The  $R_a$  of the polished steel surface was found to be 75.96 nm, while the specimen immersed in 1 M HCl was found to be 317.14 nm due to dissolution of metal. The addition of TAPU to the corrosive solutions reduced the roughness to 168.58 (5 mg/l TAPU) and 124.22 (200 mg/l TAPU) nm, respectively. The  $R_q$  values reduced to 118.08 nm (in 5 mg/l TAPU acid solution) and 85.01 nm (in 200 mg/l TAPU acid solution) from 148.21 nm (in 1 M HCl). The maximum peak depth of the specimen was reduced from 875.85 nm (1 M HCl) to 591.87 nm (5 mg/l TAPU) to 453.63 nm (200 mg/l TAPU) nm, respectively. These data indicated that the absorbed TAPU polymers provided an effective corrosion inhibition in acidic solution[35, 40].

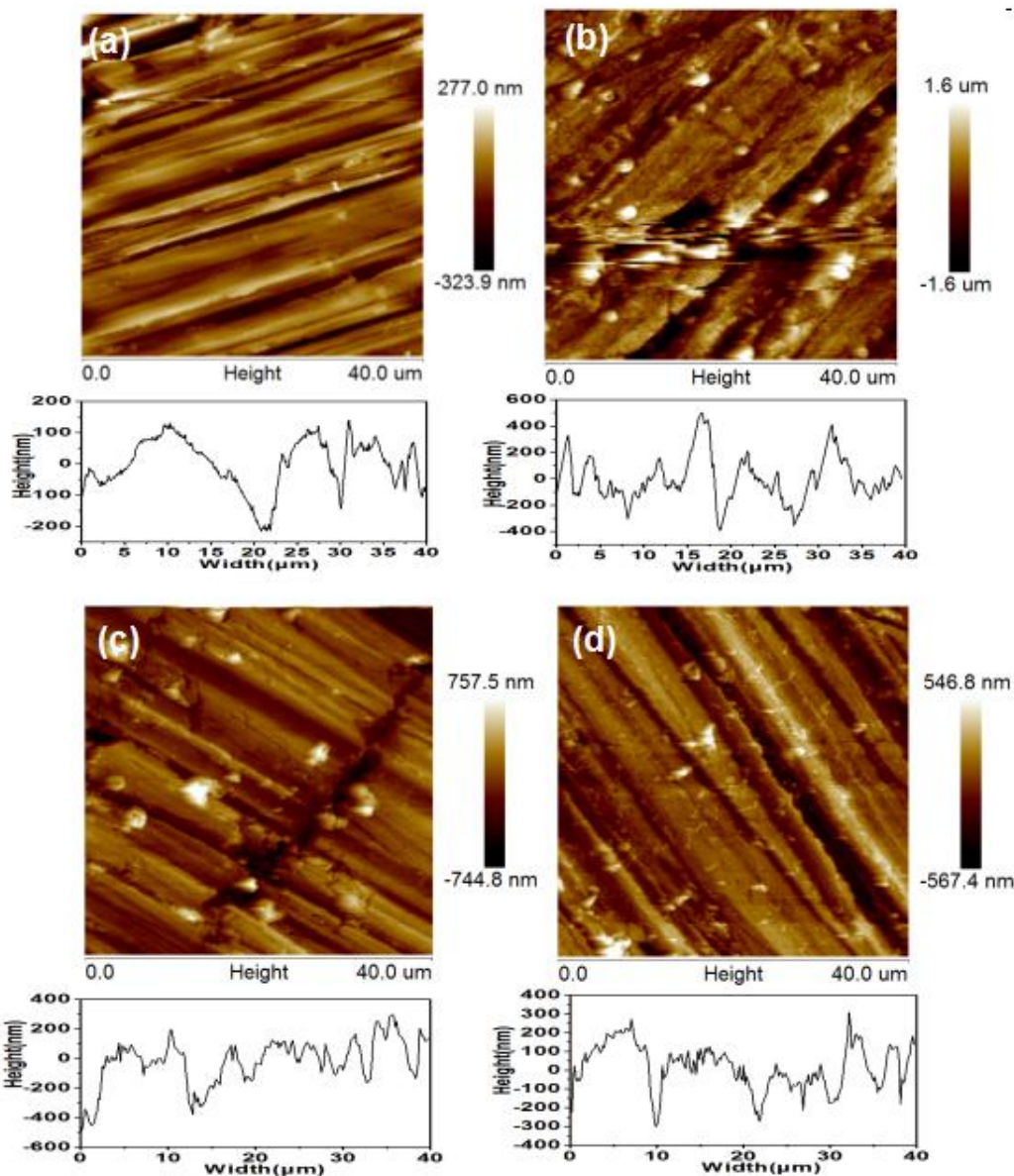


**Figure 8.** AFM images of mild steel (a) polished, (b) after immersion without inhibitor, (c) with 5 mg/l TAPU, (d) with 200 mg/l TAPU. □□□□

**Table 3.** Roughness and depth analysis data derived from AFM images from mild steel immersed in 1 M HCl in the absence and presence of TAPU.

Specimen	Average roughness $R_a$ (nm)	Root-mean-square $R_q$ (nm)	Maximum peak depth height (nm)
Bare steel	75.96	67.15	347.34
Blank (1 M HCl)	314.17	148.21	875.85
TAPU(5mg/l)	168.58	118.08	591.87
TAPU (200mg/l)	124.22	85.01	453.63

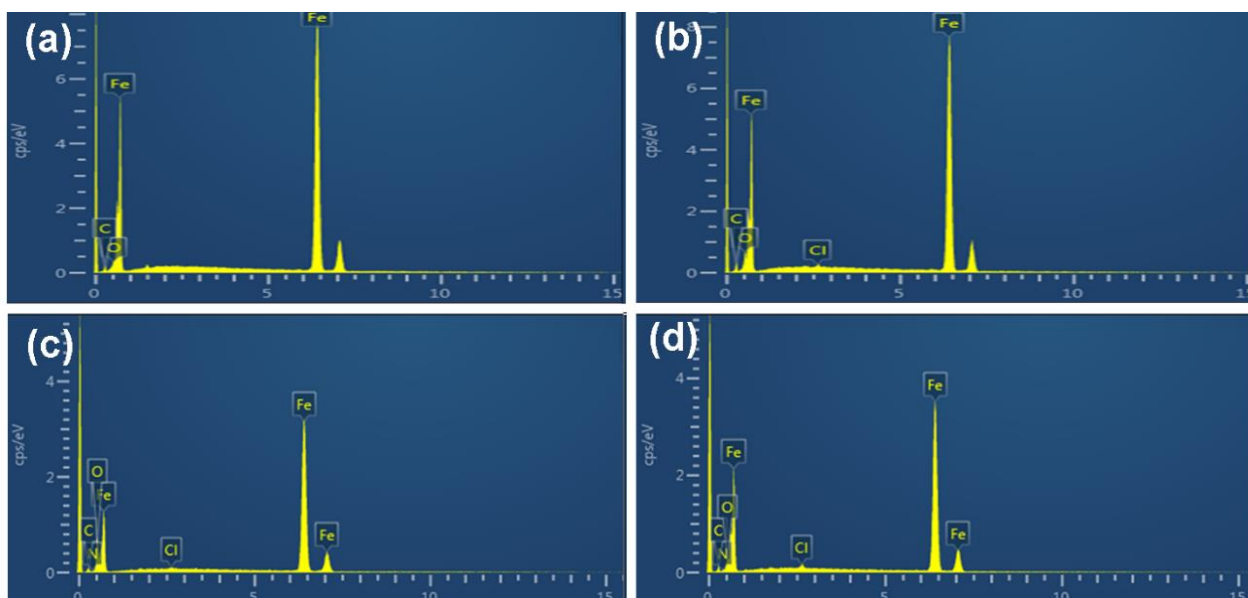


**Figure 9.** EDS spectra of mild steel specimens, (a) polished, (b) after immersion without inhibitor, (c) with 5 mg/l TAPU, (d) with 200 mg/l TAPU.

EDS analysis was used to determine the elemental composition of steel surface. As shown in Figure 9, the EDS spectra for the specimens in the presence of TAPU acidic solution showed an additional characteristic peak attributed to N from aniline trimer, indicating that TAPU molecules adsorbed on the mild steel surface[39].

#### 4. CONCLUSIONS

We have successfully synthesized trianiline containing water soluble polyurethane (TAPU) by condensation reaction of polyethylene glycol, toluene diisocyanate and amine capped trianiline. The corrosion inhibition performance of TAPU in 1 M HCl corrosive medium was investigated by various techniques including weight loss measurements, potentiodynamic polarization, EIS, adsorption isotherm, SEM/EDS, and AFM. Results confirmed that TAPU was a mixed type inhibitor and the adsorption of TAPU on the mild steel surface in 1 M HCl solution followed Langmuir adsorption isotherm. The inhibition efficiency (IE%) increased with a rise in TAPU concentration, reaching a value up to 97% at a concentration of 200 mg/l. This novel oligoaniline based polyurethane showed potential applications in some acid-based industrial processes such as acid assisted pickling, cleaning, descaling and oil well acidizing.

#### ACKNOWLEDGEMENTS

The authors gratefully appreciate financial support provided by One Hundred Talented People of the Chinese Academy of Sciences (Y60707WR04), Zhejiang Provincial Natural Science Fund (LY16B040004).

**References**

1. R. Baskar, D. Kesavan, M. Gopiraman, K. Subramanian, *Prog. Org. Coat.*, 77 (2014) 836.
2. H. Liu, T. Gu, Y. Lv, M. Asif, F. Xiong, G. Zhang, H. Liu, *Corros. Sci.*, 117 (2017) 24.
3. G. Sığircık, T. Tüken, M. Erbil, *Corros. Sci.*, 102 (2016) 437.
4. E. Gutiérrez, J. A. Rodríguez, J. Cruz-Borbolla, J. G. Alvarado-Rodríguez, P. Thangarasu, *Corros. Sci.*, 108 (2016) 23.
5. Y. G. Avdeev, Y. I. Kuznetsov, A. K. Buryak, *Corros. Sci.*, 69 (2013) 50.
6. D. Daoud, T. Douadi, H. Hamani, S. Chafaa, M. Al-Noaimi, *Corros. Sci.*, 94 (2015) 21.
7. A. Kosari, M. H. Moayed, A. Davoodi, R. Parvizi, M. Momeni, H. Eshghi, H. Moradi, *Corros. Sci.*, 78 (2014) 138.
8. J. Xu, M. Wang, N. P. Wickramaratne, M. Jaroniec, S. Dou, L. Dai, *Adv. Mater.*, 27 (2015) 2042.
9. B. D. B. Tiu, R. C. Advincula, *React. Funct. Polym.*, 95 (2015) 25.
10. Y. Liu, S. Li, J. Zhang, J. Liu, Z. Han, L. Ren, *Corros. Sci.*, 94 (2015) 190.
11. G. L. Mendonça, S. N. Costa, V. N. Freire, P. N. Casciano, A. N. Correia, P. de Lima-Neto, *Corros. Sci.*, 115 (2017) 41.
12. S. Uluata, D. J. McClements, E. A. Decker, *J. Agric. Food Chem.*, 63 (2015) 1819.
13. D. M. Gurudatt, K. N. Mohana, *Ind. Eng. Chem. Res.*, 53 (2014) 2092.
14. B. Yao, G. Wang, J. Ye, X. Li, *Mater. Lett.*, 62 (2008) 1775.
15. N. P. Tavandashiti, M. Ghorbani, A. Shojaei, J. M. C. Mol, H. Terryn, K. Baert, Y. Gonzalez-Garcia, *Corros. Sci.*, 112 (2016) 138.
16. J. A. Syed, S. Tang, H. Lu, X. Meng, *Ind. Eng. Chem. Res.*, 54 (2015) 2950.
17. L. Gu, X. Zhao, X. Tong, J. Ma, B. Chen, S. Liu, H. Zhao, H. Yu, J. Chen, *Int. J. Electrochem. Sci.*, 11 (2016) 1621.
18. L. Vacareanu, A. M. Catargiu, M. Grigoras, *J. Anal. Methods Chem.*, 2012 (2012) 737013.
19. S. Prakash, C. R. K. Rao, M. Vijayan, *Electrochim. Acta*, 53 (2008) 5704.
20. O. A. Bell, G. Wu, J. S. Haataja, F. Brommel, N. Fey, A. M. Seddon, R. L. Harniman, R. M. Richardson, O. Ikkala, X. Zhang, C. F. Faul, *J. Am. Chem. Soc.*, 137 (2015) 14288.
21. S. Yuan, S. Tang, L. Lv, B. Liang, C. Choong, S. O. Pehkonen, *Ind. Eng. Chem. Res.*, 51 (2012) 14738.
22. Y. E. Miao, G. N. Zhu, H. Hou, Y. Y. Xia, T. Liu, *J. Power Sources*, 226 (2013) 82.
23. H. Wang, P. Guo, Y. Han, *Macromol. Rapid Commun.*, 27 (2006) 63.
24. J. Gao, K. Li, W. Zhang, C. Wang, Z. Wu, Y. Ji, Y. Zhou, M. Shibata, R. Yosomiya, *Macromol. Rapid Commun.*, 20 (1999) 560.
25. R. Dong, X. Zhao, B. Guo, P. X. Ma, *ACS Appl. Mater. Inter.* 8 (2016) 17138.
26. R. Arukula, A. R. Thota, C. R. Rao, R. Narayan, B. Sreedhar, *J. Appl. Polym. Sci.*, 131 (2014).
27. H. Y. Huang, T. C. Huang, J. C. Lin, J. H. Chang, Y. T. Lee, J. M. Yeh, *Mater. Chem. Phys.*, 137 (2013) 772.
28. M. Cui, S. Ren, J. Chen, S. Liu, G. Zhang, H. Zhao, L. Wang, Q. Xue, *Appl. Surf. Sci.*, 397 (2017) 77.
29. B. Chen, J. Ma, L. Gu, S. Liu, H. Zhao, H. Yu, J. Chen, *Int. J. Electrochem. Sci.*, 10 (2015) 9154.
30. A. P. Hanza, R. Naderi, E. Kowsari, M. Sayebani, *Corros. Sci.*, 107 (2016) 96.
31. S. S. Abd El Rehim, S. M. Sayyah, M. M. El-Deeb, S. M. Kamal, R. E. Azooz, *Int. J. Ind. Chem.*, 7 (2016) 39.
32. K. R. Ansari, M. A. Quraishi, A. Singh, *Corros. Sci.*, 79 (2014) 5.
33. I. Naqvi, A. Saleemi, S. Naveed, *Int. J. Electrochem. Sci.*, 6 (2011) 146.
34. Z. Hu, Y. Meng, X. Ma, H. Zhu, J. Li, C. Li, D. Cao, *Corros. Sci.*, 112 (2016) 563.
35. [M. Yadav, T. K. Sarkar, T. Purkait, *J. Mol. Liq.*, 212 (2015) 731.
36. M. I. K. Momin, I. Bahadur, E. E. Ebenso, M. S. Islam, L. O. Olasunkanmi, D. Ramjugernath, N. A. Koorbanally, *J. Mol. Liq.*, 223 (2016) 819.

37. M. Mobin, M. Rizvi, *Carbohydr. Polym.*, 156 (2017) 202.
38. M. Yadav, D. Sharma, T. K. Sarkar, *J. Mol. Liq.*, 212 (2015) 451.
39. M. Yadav, R. R. Sinha, T. K. Sarkar, I. Bahadur, E. E. Ebenso, *J. Mol. Liq.*, 212 (2015) 686.
40. J. Telegdi, G. Luciano, S. Mahanty, T. Abohalkuma, *Mater. Corros.*, 67 (2016) 1027.

© 2017 The Authors. Published by ESG ([www.electrochemsci.org](http://www.electrochemsci.org)). This article is an open access article distributed under the terms and conditions of the Creative Commons Attribution license (<http://creativecommons.org/licenses/by/4.0/>).